

Negative resistance amplifier circuit using GaAsFET modelled single MESFET

Olasunkanmi Ojewande, Charles Ndujiuba, Adebisi A. Adelokun,
Segun I. Popoola, Aderemi A. Atayero

Department of Electrical and Information Engineering, Covenant University, Ota, Nigeria

Article Info

Article history:

Received May 31, 2018

Revised Feb 23, 2019

Accepted Mar 12, 2019

Keywords:

Conventional distributed amplifier (CDA)

Intermodulation distortion (IMD)

Negative resistance amplifier

Metal-semiconductor field-effect transistor (MESFET)

ABSTRACT

Negative resistance devices have attracted much attention in the wireless communication industry because of their low cost, better performance, high speed, and reduced power requirements. Although negative resistance circuits are non-linear circuits, they are associated with distortion, which may either be amplitude-to-amplitude distortion or amplitude-to-phase distortion. In this paper, a unique way of realizing a negative resistance amplifier is proposed using a single metal-semiconductor field-effect transistor (MESFET). Intermodulation distortion test (IMD) is performed to evaluate the characteristic response of the negative resistance circuit amplifier to different bias voltages using the harmonic balance (HB) of the advanced designed software (ADS 2016). The results obtained are compared to those of a conventional distributed amplifier. The findings of this study showed that the negative resistance amplifier spreads over a wider frequency output with reduced power requirements while the conventional distributed amplifier has a direct current (DC) offset with output voltage of 32.34 dBm.

This is an open access article under the [CC BY-SA](https://creativecommons.org/licenses/by-sa/4.0/) license.



Corresponding Author:

Olasunkanmi Ojewande,
Department of Electrical and Information Engineering,
Covenant University,
Ota, Nigeria.
Email: olasunkanmi.ojewande@stu.cu.edu.ng

1. INTRODUCTION

Wireless communication industry has continued to witness exponential growth due to recent advances in modern electronics and semiconductor technologies [1-4]. Therefore, adequate consideration must be given to high quality performance, low power consumption, cost, and size reduction in the design of electronic circuits of wireless communication systems [5]. A practical oscillator serves as energy source in microwave systems, integrated antennas, Radio Detection and Ranging (RADAR), and satellite communication systems [6]. Voltage-controlled oscillators (VCOs) is commonly used because of the significant reduction in electrical power requirements in modern communication systems [7-9].

The concept of negative differential resistance (NDR) is mostly applied to produce oscillation in wireless communication systems at a desired frequency [10, 11]. NDR is often employed in logic and memory circuits [12-14]. The resonance tunneling diode (RTD) has gathered much attention in producing an NDR characteristic in which the slope is negative in the I-V curve [15]. The circuit that uses negative differential resistance device circuits has high speed particularly when RTD is integrated with hetero-junction bipolar transistors (HBTs). Choi et al [6] showed that a negative resistance device that is enabled with HBTs will deliver high speed in most practical monolithic microwave integrated circuits

(MMICs) as obtainable in VCOs and most converters, whether analogue or digital. The current-voltage property of an NDR device can provide various steady states that have the capacity to increase the switching and memory functionality per design and circuit robustness and lower power consumption [16-18].

Negative resistance devices (NRDs) present an interesting solution by compensating for pass-band insertion loss in gain enhancers tunable applications [10, 19]. The benefits of lower cost, smaller sizes and weight authenticate the development of fully integrated Microwave systems and Radio Frequency (RF) using MMIC technologies [20-22]. The realization of NRDs using a different configuration of FET and MOSFET is proposed in [23, 24]. RF amplifiers are designed to increase a low signal to a particular power level that is sufficient in communicating from a transmitter to the receiver through space. The introduction of a large signal into an analogue systems or RF power amplifier is usually accompanied by distortion which can exhibit itself in different forms such as amplitude distortion, phase distortion or gain compression when driven by a single signal but for a two tone or multiple signal it appears as an in-band frequency or intermodulation distortion (IMD).

Intermodulation distortion is an important metrics for measuring linearity of a wide range RF microwave components [25, 26]. It describes the ratio between the powers of fundamental tones in decibel (dB). Linearity is crucial to all telecommunication devices as it can enhance the performance of a wireless communication systems. Furthermore, a single stage conventional distributed amplifier is also designed using our designed tool and the conventional distributed amplifier is also model as the negative resistance circuit amplifier by using the same gallium arsenide field-effect transistor (GaAsFET) model for metal-semiconductor field-effect Transistor (MESFET). The harmonic balance is used to perform the required frequency response of both devices to measure the intermodulation distortion at a frequency of 4 GHz to 6 GHz at a step of 100 MHz.

Intermodulation Distortion (IMD) is a very useful metrics for linearity of a wide range communication devices. The operations of IMD is performed by the introduction of a two-tone signal into the devices-under-test (DUT) such as amplifiers or pre-amplifiers specifications [27]. A linear amplifier always produces an output signal that would be two tones of the exact same frequency similar to the input signal. In this paper, a unique way of realizing a negative resistance amplifier is proposed using a single metal-semiconductor field-effect transistor (MESFET). IMD is performed to evaluate the characteristic response of the negative resistance circuit amplifier to different bias voltages using the harmonic balance (HB) of the advanced designed software (ADS 2016). The results obtained are compared to those of a conventional distributed amplifier.

2. MATERIALS AND METHODS

There are different methods of linearizing an RF power amplifier and the best method for linearization of an RF power amplifier is the pre-distortion method. This method is more prominent due to its reduction in cost and it also offers a wider range of bandwidth since it has an open loop structure and furthermore it has a low-power consumption [28-30]. The linearity performance of an RF power amplifier always depends on the nonlinear property of the amplifier. The nonlinearity behavior of an amplifier for a memory-less system can be predicted by measuring the amplitude-to-amplitude modulation and amplitude-to-phase modulation. The introduction of a two-tone signal into an RF-power amplifier is usually measured directly by the designer and the measured data is then used to determine the linearity of the amplifier. The intermodulation distortion magnitude is measured by a spectrum analyzer and the IMD's component is usually measured directly by the difference between the phase and the fundamental intermodulation components [31]. Table 1 presents the measure of intermodulation distortion of two different frequencies.

Table 1. Intermodulation distortion frequencies

Order	Frequency (w1)	Frequency (w2)	Frequency 1 (kHz)	Frequency 2 (kHz)
First	w ₁	w ₂	300	301
Second	w ₁ +w ₂	w ₂ -w ₁	601	1
Third	2w ₁ -w ₂	2w ₂ -w ₁	299	302
Fifth	3w ₁ -w ₂	3w ₂ -2w ₁	599	303
Seventh	4w ₁ -3w ₂	4w ₂ -3w ₁	297	304
Ninth	5w ₁ -4w ₂	5w ₂ -4w ₁	296	305

Let the tone-input signal of an RF-power amplifier be modelled as given by (1):

$$Z_{in}(t) = V_{in} \cos w_1(t) + V_{in} \cos w_2(t) \quad (1)$$

$$\omega_1 < \omega_2,$$

$$\omega_2 - \omega_1 = \Delta\omega$$

$$Z_{in}(t) = \frac{2V_{in}\cos(\omega_2 - \omega_1)}{2t} \cdot \frac{\cos(\omega_2 + \omega_1)}{2t} \quad (2)$$

here frequency $(\omega_2 - \omega_1)/2$ is the modulating freq ω_m , which is half of the frequency spacing between two tones. $(\omega_2 + \omega_1)/2$ is the RF center frequency.

In (2) can be written in the form of (3):

$$Z_{in}(t) = 2V_{in}\cos(\omega_m t)\cos(\omega_{cen} t) \quad (3)$$

this two-tone signal is recognize as a double side bands suppressed carrier signal having a carrier frequency ω_{cen} and modulating frequency ω_m . When the signal is applied to a power amplifier the output signal can be expressed as given by (4):

$$Z_o(t) = \sum_0^k ak[V(t)\cos\omega_1 t + V(t)\cos\omega_2 t] \quad (4)$$

simplifying in (4) will always result in new frequency components which reveals the non-linearity of the device known as the intermodulation distortion. For a two tone signal the IMD can be obtained using (5):

$$\omega_{new} = [\pm p\omega_1 \pm q\omega_2]$$

where p and q are integers are positive zero inclusive.

$p + q = k$ denotes the order of the IMD.

The intermodulation product for two frequencies (ω_1 and ω_2) for different order can be obtained as follows:

- $(\omega_1 + \omega_2)$ is the second order
- $(2\omega_1 - \omega_2)$ is the third order
- $(3\omega_1 - 2\omega_2)$ is the fifth order

given the two frequencies (ω_1 and ω_2) as 300 kHz and 301 kHz respectively, which are 1 kHz apart. The odd order products are nearer or closest to the fundamental frequency ω_1 and ω_2 . The one-third order is 1 kHz lower above ω_2 and 2 kHz above ω_1 .

A typical negative resistance amplifier is shown in Figure 1. The negative resistance amplifier circuit was designed and modelled using a gallium arsenide field-effect transistor (GaAsFET) on the ADS simulation software. The drain of the MESFET is properly grounded while the source and gate are lumped with component of resistors and capacitors and inductor, The source R_2 is used to bias the circuit in other to set the DC operating point, by providing an automatic transient protection and also to reduce the variation of the effects of the drain current I_{ds} and the temperature. The capacitor C_2 is used as a capacitive serial feedback. The negative resistance amplifier is biased with a voltage of 20.5 Vdc.

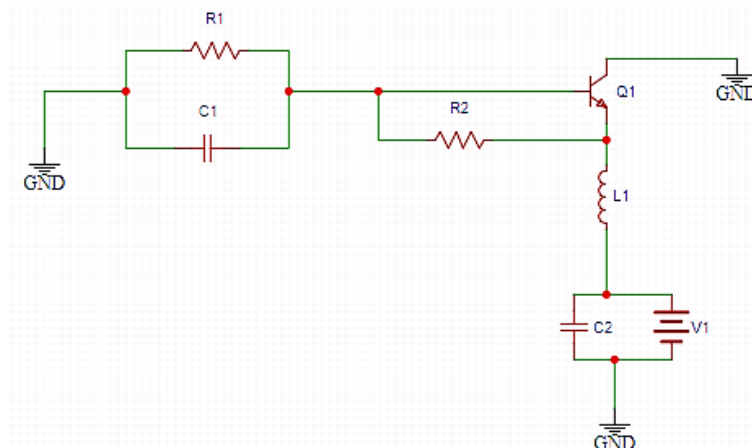


Figure 1. Negative resistance amplifier circuit

2.1. Small signal analysis of negative resistance amplifier circuit using MESFET model

The designed negative resistance amplifier was developed using MESFET model, and the general parameters are given as listed below and represented in the Figure 2. The impedance analysis of the negative resistance amplifier is described in Figure 3. The input impedance of the negative resistance amplifier circuit is given by (13).

$$I_{in} = I_1 + I_2 \tag{5}$$

$$I_1 = Vin / (Z1 + R1) \tag{6}$$

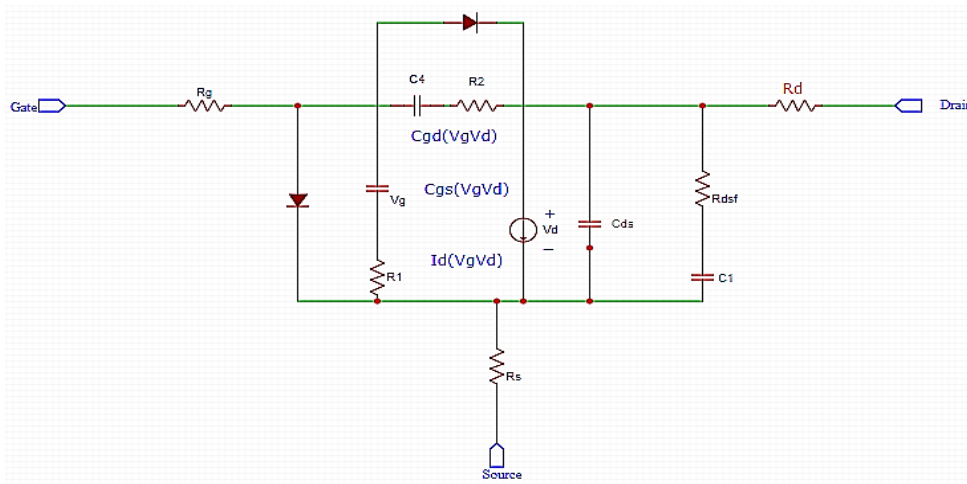


Figure 2. MESFET model

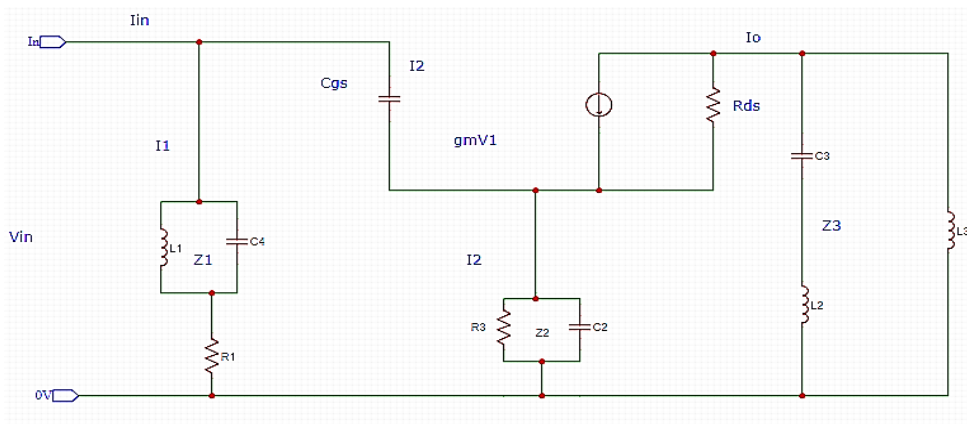


Figure 3. Negative resistance amplifier circuit

The impedance across L1//C1,

$$Z_1 = j\omega L_1 / (1 - \omega^2 L_1 C_1) = jX_1 \tag{7}$$

the voltage V_1 is developed across the gate to source capacitance:

$$v_1 = I_2 Z_{gs} = I_{in} - \frac{V_{in}}{Z_1 + R_1} Z_{gs} \tag{8}$$

$$V_2 = (I_2 + I_o) Z_2 = V_{in} - (I_{in} - \frac{V_{in}}{Z_1 + R_1}) \tag{9}$$

$$I_o = gmV_1 + \frac{V_2 + I_o Z_3}{R_{ds}} = (gmV_1 R_{ds} + V_2) / R_{ds} - Z_3 \tag{10}$$

$$V_2 = \frac{Z_2((I_{in}(Z_1+R_1)-V_{in})(R_{ds}-Z_3+g_m X_{gs} R_{ds}))}{(Z_1+R_1)(R_{ds}-Z_3-Z_2)} \quad (11)$$

$$= V_{in} \left(I_{in} - \frac{V_{in}}{Z_1+R_1} \right) X_{gs} \quad (12)$$

$$Z_{in} = \frac{V_{in}}{I_{in}} = \frac{Z_2(Z_1+R_1)(R_{ds}-Z_3+g_m X_{gs} R_{ds}) + (Z_1+R_1)(R_{ds}-Z_3-Z_2)}{(Z_1+R_1+X_{gs})(R_{ds}-Z_3-Z_2) + Z_2(R_{ds}-Z_3+g_m X_{gs} R_{ds})} \quad (13)$$

$$Z_2 = (R_2 - j\omega C_2 R_2^2) / (1 - \omega^2 C_2^2 R_2^2) = R - jX_2 \quad (14)$$

$$Z_3 = \frac{j\omega C_3(L_3 - \omega^2 L_2 L_3 C_3)}{C_3(1 - \omega^2 L_2 C_3(L_2 + L_3))} = jX_3 \quad (15)$$

$$Z_{in} = \text{Re}(Z_{in}) + j\text{Im}(Z_{in}) = R_n + jX \quad (16)$$

- Rs = Ohmic source resistance
- Rd = Ohmic drain resistance
- Rg = Ohmic gate resistance
- R₁ = Semiconductor resistance
- Cds = Drain-to-source capacitance
- Cgs = Gate-to-source capacitance
- Id = Linear current source
- Vgs = External gate-to-source voltage.
- V_x = Internal channel voltages for drain and source
- Vds = External drain-to-source voltage
- Vgd = External gate-to-drain voltage

2.2. Simulation of negative resistance amplifier

The N-type GaAsFET MESFET is used to realize the negative resistance amplifier circuit, which is a one port network and in order to simulate the behavior of the negative resistance amplifier and the IMD. The following steps are used to realize the negative resistance amplifier using ADS as shown in Figure 4. Firstly, the designed amplifier is a one port network and in other to be able to simulate accordingly using the ADS it has to be converted to a port network as shown in Figure 5, the drain of the amplifier is properly grounded, the gate is also lumped with a series inductor and in parallel with resistor and capacitor with value been selected carefully.

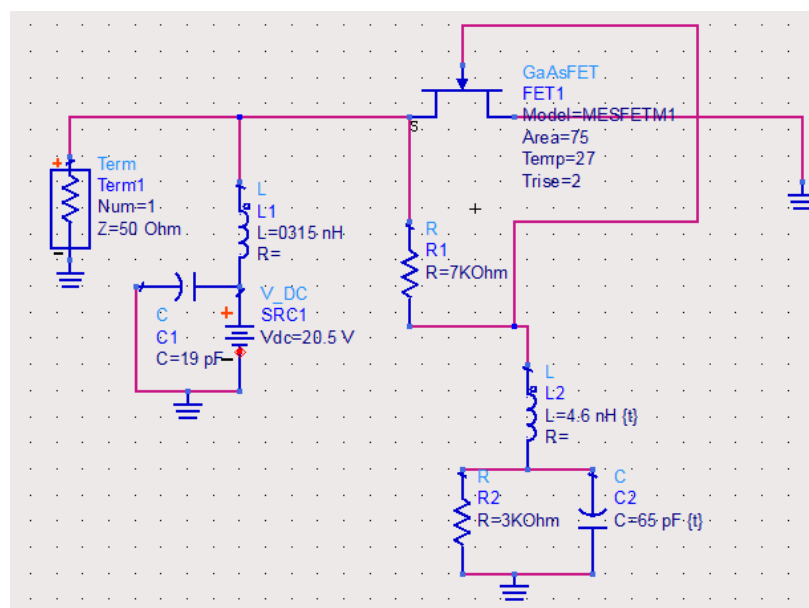


Figure 4. Negative resistance amplifier design using ADS

Secondly, Figure 5 was converted to a box type negative resistance NR_1 coupled with the circulator in the ADS software. The circulator enhances a lossless power match for coupling the signal and in like manner provides an input and an output terminal for the negative resistance amplifier circuit. The second port of the circulator is connected with the source input say the P_ntone signal coupled with a current probe while port three is also connected to another current probe and terminated with a 50Ω resistor transmission line, and then grounded accordingly. The nth-order determine the number of the input signal which is either a single tone signal or a two-tone signal.

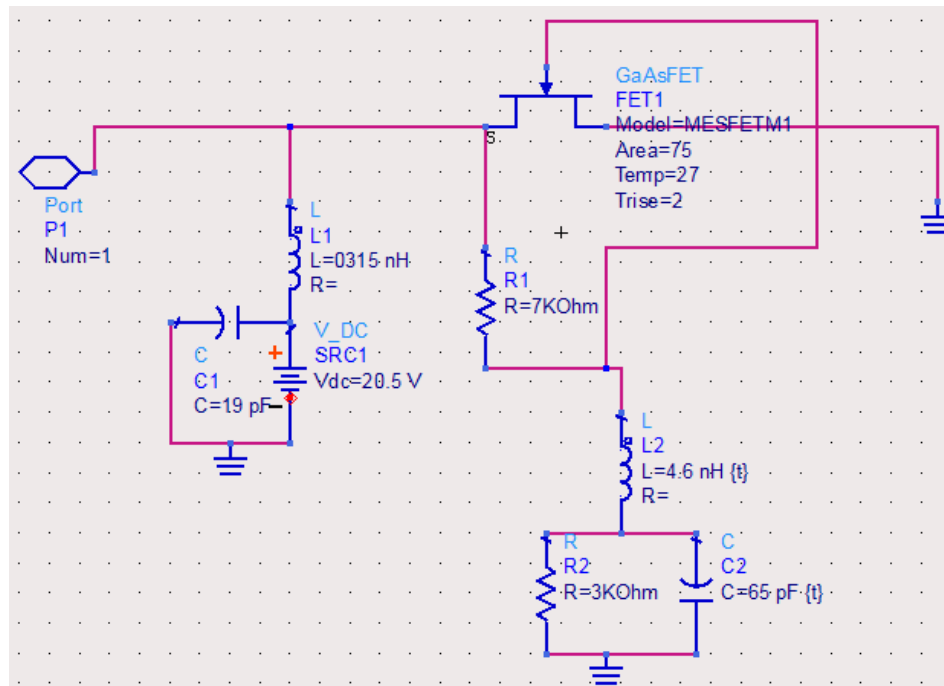


Figure 5. Port conversion

Introducing a p_ntone signal into the designed oscillator or amplifier which serves as the source to the amplifier, a probe is connected to vary the input signal while the second terminal of the probe is connected to port one of the circulator to serve as the source input signal, then the designed one port negative resistance amplifier is connected to the second port of the circulator. The port three of the circulator is used as the output port where a probe 1 is connected and is terminated with a 50Ω resistance as the transmission line constant, The negative resistance amplifier input and the output port is labeled as V_{in} and V_{out} with respect to the terminal of the probe to be used in varying the input and the output signal.

As for the input signal to the negative resistance amplifier, n represents the number of input signal, when n is set to one it represents single tone and when n is set to 2, it is called two tone signals. The ADS have a special way of setting the input power which can be converted either to polar form in dBm or to Watt, the use of dbm to watt is been employed. The harmonic representation in HB that is embedded in the ADS tool is used to obtain the steady state response of the frequency components of the negative resistance amplifier, it is commonly used than the traditional time domain methods. The frequency steps are also set as shown in Table 1. The HB is also used to measure the intermodulation distortion of the negative the resistance amplifier which determine the amplifier linearity.

The designed conventional distributed amplifier is shown in the Figure 6 with the GaAs MESFET model similar to that of the negative resistance amplifier having two different probes to control the input signal of the conventional distributed amplifier, it is biased in a stable state having a termination of 50Ω impedance without which there will be no response for both conventional amplifiers and the NRA. A p_ntone signal is attached to the input of the amplifier in order to determine the response of the output signal when a single tone signal is introduced into the CDA by setting the value of n to either one or two the emphasis here is two tone signals. Then the output of the signal can then be verifying and compared to that of the negative resistance amplifier.

The designed conventional distributed amplifier is shown in the Figure 6 with the GaAs MESFET model similar to that of the negative resistance amplifier having two different probes to control the input signal of the conventional distributed amplifier, it is biased in a stable state having a termination of 50Ω impedance without which there will be no response for both conventional amplifiers and the NRA. A p_tone signal is attached to the input of the amplifier in order to determine the response of the output signal when a single tone signal is introduced into the CDA by setting the value of n to either one or two the emphasis here is two tone signals. Then the output of the signal can then be verifying and compared to that of the negative resistance amplifier.

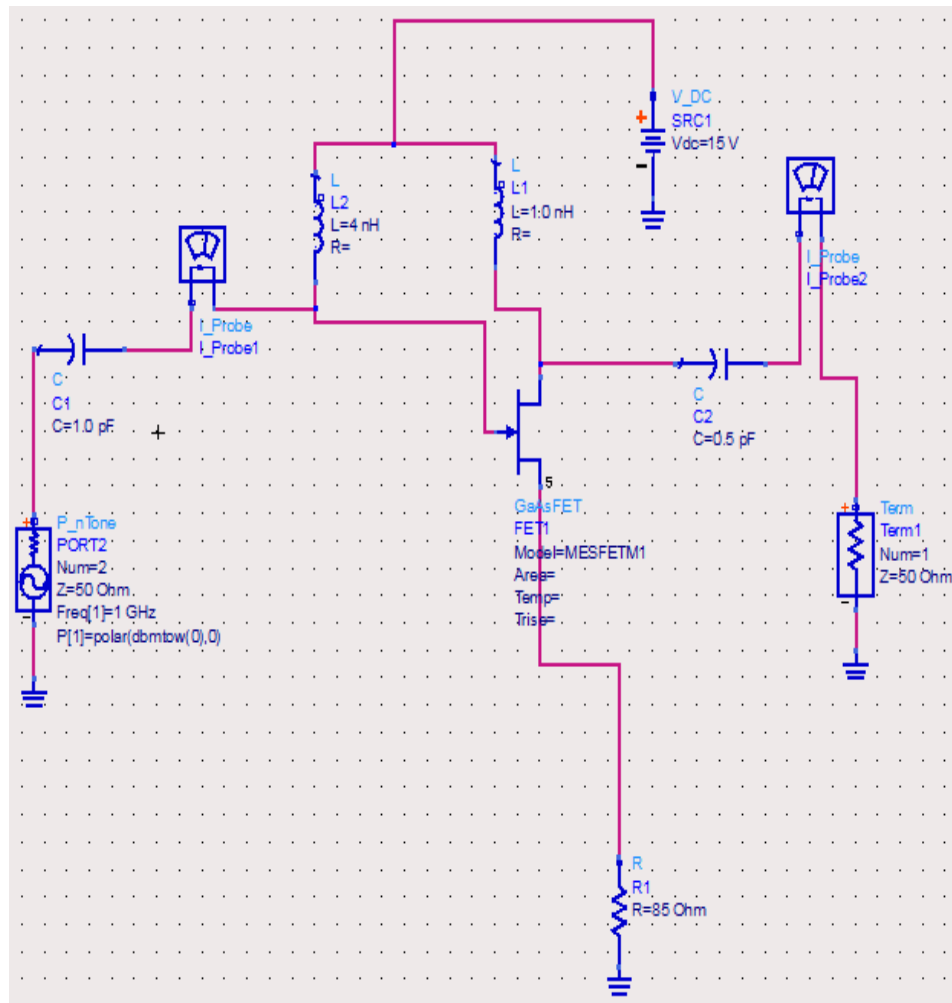


Figure 6. Schematic design for a conventional distributed amplifier using ADS

3. RESULTS AND DISCUSSIONS

The designed negative resistance amplifier behaviour is obtained and shown in the Figure 7 using the ADS simulation tool, the frequency range that is used ranges from (4.0 to 6.0 GHz) while at frequency above 6 GHz is shown in Figure 8. The two figures show the real and the imaginary of the impedance plot to the selected frequency. The GaAsFET MESFET is usually required for higher frequencies and it performs excellently at above 5 GHz [13]. Figure 9 shows the gain stability of the negative resistance amplifier. The gain of the negative resistance is plotted against a wider range of RF input power in dBm. The negative resistance amplifier is more stable than that of the conventional amplifier. The conventional amplifier is also designed and modeled in a similar way as that of the negative resistance amplifier using a single stage GaAsFET MESFET. Figure 10 shows the behavior of a conventional distributed amplifier gain against the RF input power; the graph appears to have a ripple at RF input from -90.000 to -100.000 dbm at a gain of -18.37857.

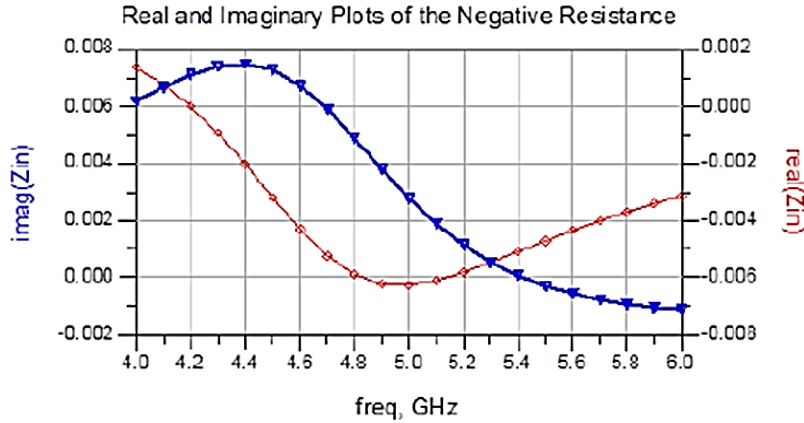


Figure 7. Plot of negative resistance amplifier circuit response at 6 GHz

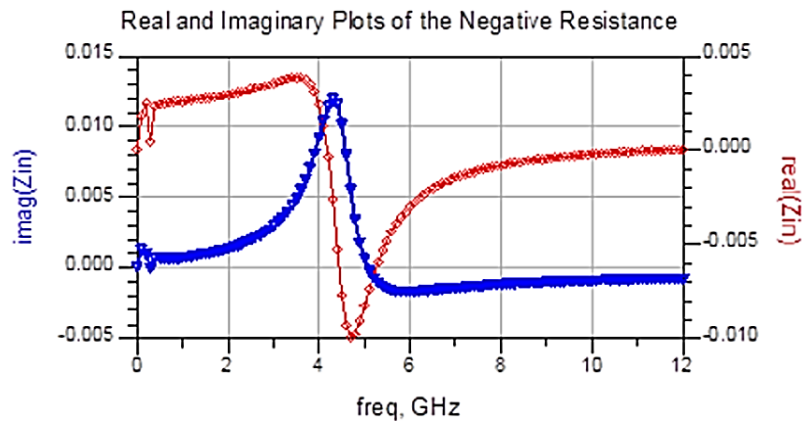


Figure 8. Plot of negative resistance amplifier circuit response above 6 GHz



Figure 9. Gain stability of negative resistance amplifier against RF input power

When the p_ntone signal is set to either a single tone or a two-tone signal and is fed into the negative resistance amplifier, the output response is shown in Figure 11 for single tone while Figure 12 shows that of the two-tone signal having different fundamental frequency and a DC offset. The y-axis represents the power output in dbm (V_{out}) while the x-axis represents the frequency in GHz of the negative resistance amplifier. The harmonic balance is used to obtain the frequency components of the negative resistance amplifier, eight harmonics appears with different spectral line. ADS marker is used to obtain the magnitude of the output power in dbm. The single tone input signal is achieved when the p_ntone signal

is set to n value of 1, the output of the signal display seven (7) different harmonics, having a dc offset of zero and a V_{output} of 35.56 dBm which have significant effect on the performance of any wireless or communication device as shown in Figure 11. The two tone signal is achieved when the p_tone signal is introduced to the negative resistance amplifier, the n-value of the signal is set to 2, and the harmonic balance presents the frequency components as shown in the diagram, about eighteen different harmonics appears in the Table 2 having no DC offset.

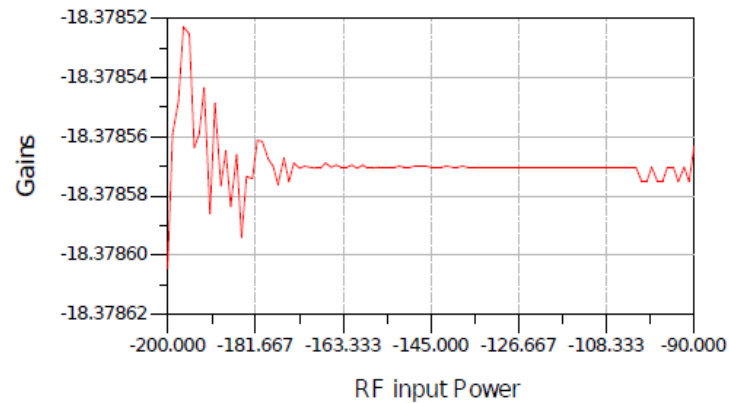


Figure 10. Gain stability of conventional distributed amplifier

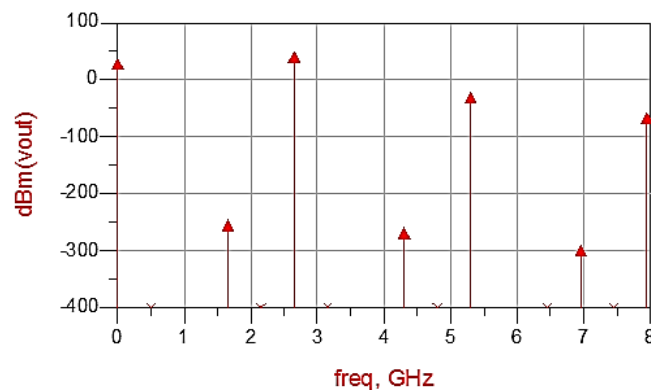


Figure 11. Single tone negative resistance amplifier using ADS

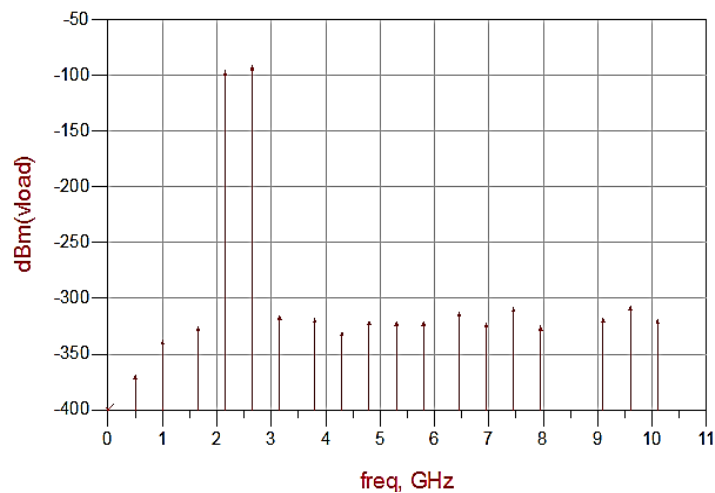


Figure 12. Two-tone input signal for the negative resistance amplifier

The two (2) tone input signal for the negative resistance amplifier have a fundamental frequency of 500 MHz the power output for the negative resistance amplifier has no DC output offset since the fundamental frequency begins with 500 MHz and the output power begins at a power output ranging from -368.563 dBm to the peak value of 10.10 GHz at a power output of -318.689 dbm. The third order intermodulation for the NRA appears to have a frequency of 4.300 GHz with an output power of -330.028 dBm. The fundamental frequency for the negative resistance device is not widely spaced as compared to the conventional distributed amplifier has this makes the negative resistance device to be more linear than the conventional distributed amplifier. Table 2 also shows the output power in dBm for the various frequencies.

Figure 13 shows the two tone input signal for the conventional distributed amplifier, the two-tone signal output has a dc offset as shown in Table 3, the dc offset has a power output of 32.34 dBm, the fundamental frequency (w_1) is at 500 MHz and the second frequency shift has a two tone signal of 2.1 GHz and 2.6 GHz both is having a marked power output of 50 dbm respectively. The third order intermodulation distortion for CDA at frequency of 4,300 MHz has a dBm output power of (-20.00 dBm). These discrepancies between the output dBm of the CDA and negative resistance amplifier is as a result of the bias voltages for the negative resistance amplifier. The distance between the fundamental frequencies for conventional distributed amplifier are widely spaced. The power output for the second order intermodulation distortion exist at a frequency of 2.100 GHz and 2.600 GHz happens to have a power output in 50.000 dBm respectively.

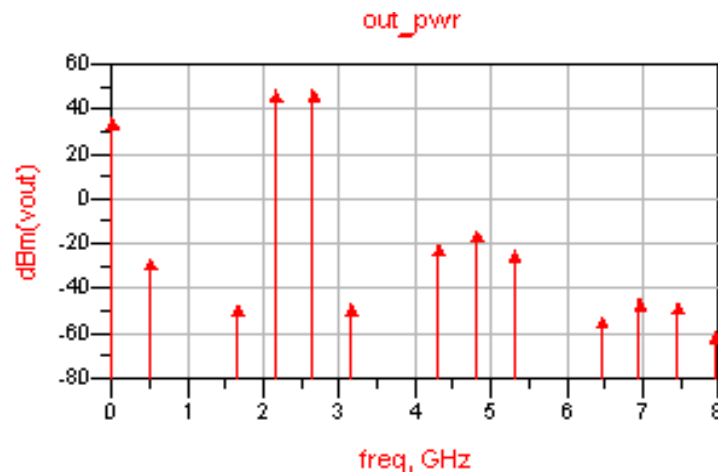


Figure 13. Two-tone signal for the conventional distributed amplifier using ADS

Table 2. Two-tone signal output for negative resistance amplifier output

S/No	Description	Frequency (m1)	Dbm (Vout)
1	Fundamental	500.0 MHz	-368.563
2	First order	1.000 GHz	-337.557
3	Second order	1.650 GHz	-325.329
4	Second order	2.150 GHz	-95.933
5	Second order	2.650 GHz	-91.061
6	Second order	3.150 GHz	-315.144
7	Third order	3.800 GHz	-318.087
8	Third order	4.300 GHz	-330.028
9	Third order	4.800 GHz	-320.171
10	Third order	5.300 GHz	-320.538
11	Third order	5.800 GHz	-320.535
12	Fourth order	6.450 GHz	-312.606
13	Fourth order	6.950 GHz	-322.249
14	Fourth order	7.450 GHz	-308.127
15	Fourth order	7.950 GHz	-324.627
16	Fifth order	9.100 GHz	-317.609
17	Fifth order	9.600 GHz	-306.750
18	Fifth order	10.100 GHz	-318.689

Table 3. Two-tone signal for the conventional distributed amplifier using ADS

S/N	Description/Order	Frequency	Vout (dm)
1	DC offset	0	32.34
2	Fundamental	500	-31,024
3	First order	1.600	-50,213
4	Second order	2.100	50,000
5	Second order	2.600	50,000
6	Second order	3.100	-50,213
7	Third order	4.300	-20.00
8	Third order	4.800	-18,534
9	Third order	5.300	-21,673
10	Fourth order	6.400	-58,230
11	Fourth order	6.900	-48,682
12	fourth order	7.400	-47,734
13	Fourth order	7.950	-60,010

4. CONCLUSION

The advanced design system software has been used to simulate the behavior of a negative resistance amplifier, the negative resistance amplifier intermodulation distortion is influenced by the various biased voltages and it presents a lower power output in dBm. The fundamental frequency for the two-tone signal of the negative resistance amplifier is more compact than that of the conventional distributed amplifier hence the negative resistance circuit is more linear than that of the conventional amplifier which is widely spaced.

The negative resistance amplifier also demonstrated a stable gain over a wider range of RF input power in dBm faster than when compared with the conventional distributed amplifier that has significant ripple effects. The negative resistance amplifier when it is perfectly realized with the appropriate bias voltage, can be used as a promising resolution to improve the nonlinearity that is usually present in most RF power amplifier in the communication or wireless industries. It is worthy of note that the bias voltage for a negative resistance device needs to be well observed as this can affect the performance of any negative resistance amplifier device.

REFERENCES

- [1] J. G. Pellerin, "Dimensions of innovation to enable the next era of intelligent systems," *2017 IEEE Electron Devices Technology and Manufacturing Conference (EDTM)*, pp. 1-1, 2017.
- [2] J. F. O'Hara, S. Ekin, W. Choi, and I. Song, "A Perspective on Terahertz Next-Generation Wireless Communications," *Technologies*, vol. 7, no. 2, pp. 1-18, 2019.
- [3] V. Biryukov, V. Vaks, K. Kisilenko, A. Panin, S. Pripolzin, A. Raevsky, *et al.*, "Development of Wireless Communication Systems in the Subterahertz Frequency Range," *Radiophysics and Quantum Electronics*, vol. 61, pp. 763-772, 2019.
- [4] M. C. Hsieh, "Advanced flip chip package on package technology for mobile applications," *2016 17th International Conference on Electronic Packaging Technology (ICEPT)*, pp. 486-491, 2016.
- [5] U. L. Rohde and A. K. Poddar, "RF-MEMS enabled RF-signal source for low-power consumption ultrawideband communication systems," *2006 IEEE International Conference on Ultra-Wideband*, pp. 113-118, 2006.
- [6] A. El'chaninov, A. I. Klimov, O. Koval'chuk, G. Mesyats, I. Romanchenko, V. Rostov, *et al.*, "Coherent summation of power of nanosecond relativistic microwave oscillators," *Technical Physics*, vol. 56, no. 1, pp. 121-126, 2011.
- [7] J. Craninckx and M. Steyaert, "Low-noise voltage-controlled oscillators using enhanced LC-tanks," *IEEE Transactions on Circuits and Systems II: Analog and Digital Signal Processing*, vol. 42, no. 12, pp. 794-804, 1995.
- [8] H. H. Hsieh and L. H. Lu, "A high-performance CMOS voltage-controlled oscillator for ultra-low-voltage operations," *IEEE Transactions on Microwave Theory and Techniques*, vol. 55, no. 3, pp. 467-473, 2007.
- [9] A. B. Khan, J. Cardenas, L. Chen, M. Khan, and A. Qureshi, "A Low Power and Low Noise Voltage-Controlled Oscillator in 28-nm FDSOI Technology for Wireless Communication Applications," *2019 IEEE Canadian Conference of Electrical and Computer Engineering (CCECE)*, pp. 1-5, 2019.
- [10] Z. Xiao, C. Ma, J. Huang, L. Liang, W. Lu, K. Hong, *et al.*, "Design of Atomically Precise Nanoscale Negative Differential Resistance Devices," *Advanced Theory and Simulations*, vol. 2, no. 2, pp. 1-18, 2019.
- [11] M. M. Salman, M. Patzauer, D. Koster, F. La Mantia, and K. Krischer, "Electro-oxidation of p-silicon in fluoride-containing electrolyte: a physical model for the regime of negative differential resistance," *The European Physical Journal Special Topics*, vol. 227, no. 18, pp. 2641-2658, 2019.
- [12] C. Heij, D. Dixon, P. Hadley, and J. Mooij, "Negative differential resistance due to single-electron switching," *Applied Physics Letters*, vol. 74, pp. 1042-1044, 1999.
- [13] S. L. Chen, P. B. Griffin, and J. D. Plummer, "Negative differential resistance circuit design and memory applications," *IEEE Transactions on Electron Devices*, vol. 56, no. 4, pp. 634-640, 2009.

- [14] S. Mohan, P. Mazumder, G. Haddad, R. Mains, and J. Sun, "Logic design based on negative differential resistance characteristics of quantum electronic devices," *IEE Proceedings G (Circuits, Devices and Systems)*, vol. 140, no. 6, pp. 383-391, 1993.
- [15] J. P. Sun, G. I. Haddad, P. Mazumder, and J. N. Schulman, "Resonant tunneling diodes: Models and properties," *Proceedings of the IEEE*, vol. 86, no. 4, pp. 641-660, 1998.
- [16] B. Cho, S. Song, Y. Ji, T. W. Kim, and T. Lee, "Organic resistive memory devices: performance enhancement, integration, and advanced architectures," *Advanced Functional Materials*, vol. 21, no. 15, pp. 2806-2829, 2011.
- [17] S. T. Han, Y. Zhou, and V. Roy, "Towards the development of flexible non-volatile memories," *Advanced Materials*, vol. 25, no. 38, pp. 5425-5449, 2013.
- [18] M. Haselman and S. Hauck, "The future of integrated circuits: A survey of nanoelectronics," *Proceedings of the IEEE*, vol. 98, no. 1, pp. 11-38, 2009.
- [19] Y. Wu, H. Fu, A. Roy, P. Song, Y. Lin, O. Kizilkaya, *et al.*, "Facile one-pot synthesis of 3D graphite-SiO₂ composite foam for negative resistance devices," *RSC Advances*, vol. 7, pp. 41812-41818, 2017.
- [20] C. F. Campbell, "A fully integrated Ku-band Doherty amplifier MMIC," *IEEE Microwave and Guided Wave Letters*, vol. 9, no. 3, pp. 114-116, 1999.
- [21] S. Iezekiel, M. Burla, J. Klamkin, D. Marpaung, and J. Capmany, "RF engineering meets optoelectronics: Progress in integrated microwave photonics," *IEEE Microwave Magazine*, vol. 16, no. 8, pp. 28-45, 2015.
- [22] J. Champion, A. Hassona, Z. S. He, B. Beuerle, A. Gomez-Torrent, U. Shah, *et al.*, "Toward industrial exploitation of THz frequencies: Integration of SiGe MMICs in silicon-micromachined waveguide systems," *IEEE Transactions on Terahertz Science and Technology*, vol. 9, no. 6, pp. 624-636, 2019.
- [23] L. Chua, J. Yu, and Y. Yu, "Bipolar-JFET-MOSFET negative resistance devices," *IEEE Transactions on Circuits and Systems*, vol. 32, no. 1, pp. 46-61, 1985.
- [24] H. Takagi and G. Kano, "Complementary JFET negative-resistance devices," *IEEE Journal of Solid-State Circuits*, vol. 10, no. 6, pp. 509-515, 1975.
- [25] J. C. Pedro and N. B. De Carvalho, "On the use of multitone techniques for assessing RF components' intermodulation distortion," *IEEE Transactions on Microwave Theory and Techniques*, vol. 47, no. 12, pp. 2393-2402, 1999.
- [26] M. P. Van Der Heijden, H. C. De Graaff, and L. C. De Vreede, "A novel frequency-independent third-order intermodulation distortion cancellation technique for BJT amplifiers," *IEEE Journal of Solid-State Circuits*, vol. 37, no. 9, pp. 1176-1183, 2002.
- [27] M. Krüger, F. N. Nils, and H. Reichl, "Intermodulation distortion as indicator for interconnect degradation," *2010 Proceedings 60th Electronic Components and Technology Conference (ECTC)*, pp. 477-483, 2010.
- [28] C. Chen, S. Lee, V. V. Deshpande, G.-H. Lee, M. Lekas, K. Shepard, *et al.*, "Graphene mechanical oscillators with tunable frequency," *Nature nanotechnology*, vol. 8, pp. 923-927, 2013.
- [29] C. C. Yu and K. Chang, "Novel compact elliptic-function narrow-band bandpass filters using microstrip open-loop resonators with coupled and crossing lines," *IEEE Transactions on Microwave Theory and Techniques*, vol. 46, no. 7, pp. 952-958, 1998.
- [30] L. H. Hsieh and K. Chang, "High-efficiency piezoelectric-transducer-tuned feedback microstrip ring-resonator oscillators operating at high resonant frequencies," *IEEE transactions on microwave theory and techniques*, vol. 51, no. 4, pp. 1141-1145, 2003.
- [31] I. Angelov, V. Desmaris, K. Dynefors, P. Nilsson, N. Rorsman, and H. Zirath, "On the large-signal modelling of AlGaIn/GaN HEMTs and SiC MESFETs," in *Gallium Arsenide and Other Semiconductor Application Symposium, 2005. EGAAS 2005. European*, pp. 309-312, 2005.